

Cite this: *Chem. Sci.*, 2023, 14, 8279

All publication charges for this article have been paid for by the Royal Society of Chemistry

Received 31st March 2023
Accepted 3rd July 2023

DOI: 10.1039/d3sc01670f

rsc.li/chemical-science

Macrocyclization *via* remote *meta*-selective C–H olefination using a practical indolyl template†

Pengfei Zhang,^a Zhiwei Jiang,^a Zhoulong Fan,^b Guoshuai Li,^a Qingxue Ma,^a Jun Huang,^c Jinghong Tang,^c Xiaohua Xu,^{*a} Jin-Quan Yu^{†b} and Zhong Jin^{†ac}

The synthesis of macrocyclic compounds with different sizes and linkages remains a great challenge *via* transition metal-catalysed intramolecular C–H activation. Herein, we disclose an efficient macrocyclization strategy *via* Pd-catalysed remote *meta*-C–H olefination using a practical indolyl template. This approach was successfully employed to access macrolides and coumarins. In addition, the intermolecular *meta*-C–H olefination also worked well and was exemplified by the synthesis of antitumor drug belinostat from inexpensive and readily available benzenesulfonyl chloride. Notably, catalytic copper acetate and molecular oxygen were used in place of silver salts as oxidants. Furthermore, for the first time, the formation of a macrocyclophane cyclopalladated intermediate was detected through *in situ* Fourier-transform infrared monitoring experiments and ESI-MS.

Introduction

Achieving site selectivity in C–H bond functionalization reactions is particularly important for the late-stage diversification of drug molecules.¹ With the use of diverse directing groups (DG), the activation of *ortho*-C–H bonds in arenes has been achieved *via* a conformationally rigid five- or six-membered ring transition state, *i.e.* proximity-driven cyclometalation process.² However, this approach is incapable of accessing remote *meta* or *para* C–H bonds, which are spatially and geometrically inaccessible with *ortho*-directing groups. The development of new strategies for transition metal-catalysed distal C–H bond functionalization of arenes remains a significant challenge.³ Advances⁴ in directing template (DT) strategies harnessing the understanding of distance and geometry between the target C–H bond and DG have provided a reliable solution to the problem.⁵ Through tuning of a template's spatial and geometric parameters, distal C–H bonds locating at the *meta* or *para* position of the existing functional group could be selectively activated by forming a macrocyclophane (MCP)-like pre-transition state.⁶

Bioactive macrocycles, possessing increased conformational flexibility, larger size, and extended surface area relative to traditional small-molecule drugs, show unique and potentially valuable binding properties towards therapeutic targets (Fig. 1a).⁷ As a consequence, the efficient synthesis, precise structural modification, and versatile derivatization of macrocycles are of great importance in the drug discovery process. Recently, synthetic methods for expanding the structural diversity of macrocycles, such as the construction of combinatorial libraries incorporating aromatic residue(s) in the macrocyclic backbone, have received intensive interest from the synthetic and medicinal chemistry communities (Fig. 1b).⁸ Despite this advance, development of macrocyclization strategies for construction of structurally diverse macrocycle libraries remains underexplored.⁹ The intramolecular *meta*-selective C–H functionalization to access aromatic macrocycle compounds from a linear precursor would be a highly direct, expedient, and modular method for the preparation of medicinally active macrocycles, yet this strategy has hitherto not been realized.

Inspired by the intriguing biological properties of macrocycle derivatives, we envisioned whether we could achieve a general approach to the synthesis of structurally unique macrocycle libraries through transition metal-catalysed remote *meta*-selective C–H functionalization. Macrocycles containing an aromatic moiety in their backbones would have planar, relatively rigid conformations, as well as large transannular strain, and thus should display remarkably different properties compared with other macrocycle counterparts.¹⁰

Since aryl sulfonic acids and sulfonamides are ubiquitous structural motifs widely present in pharmaceuticals, agrochemicals and other fine chemicals,¹¹ we initially selected aryl sulfonic acids as the substrate for preparing macrocycle

^aCollege of Chemistry, State Key Laboratory of Elemento-organic Chemistry, Nankai University, Tianjin 300071, China. E-mail: zjin@nankai.edu.cn

^bDepartment of Chemistry, The Scripps Research Institute, La Jolla, CA 92037, United States. E-mail: yu200@scripps.edu

^cKey Laboratory of Xinjiang Native Medicinal and Edible Plant Resource Chemistry, College of Chemistry and Environmental Sciences, Kashi University, Kashgar 844007, China

† Electronic supplementary information (ESI) available. CCDC 2142546. For ESI and crystallographic data in CIF or other electronic format see DOI: <https://doi.org/10.1039/d3sc01670f>



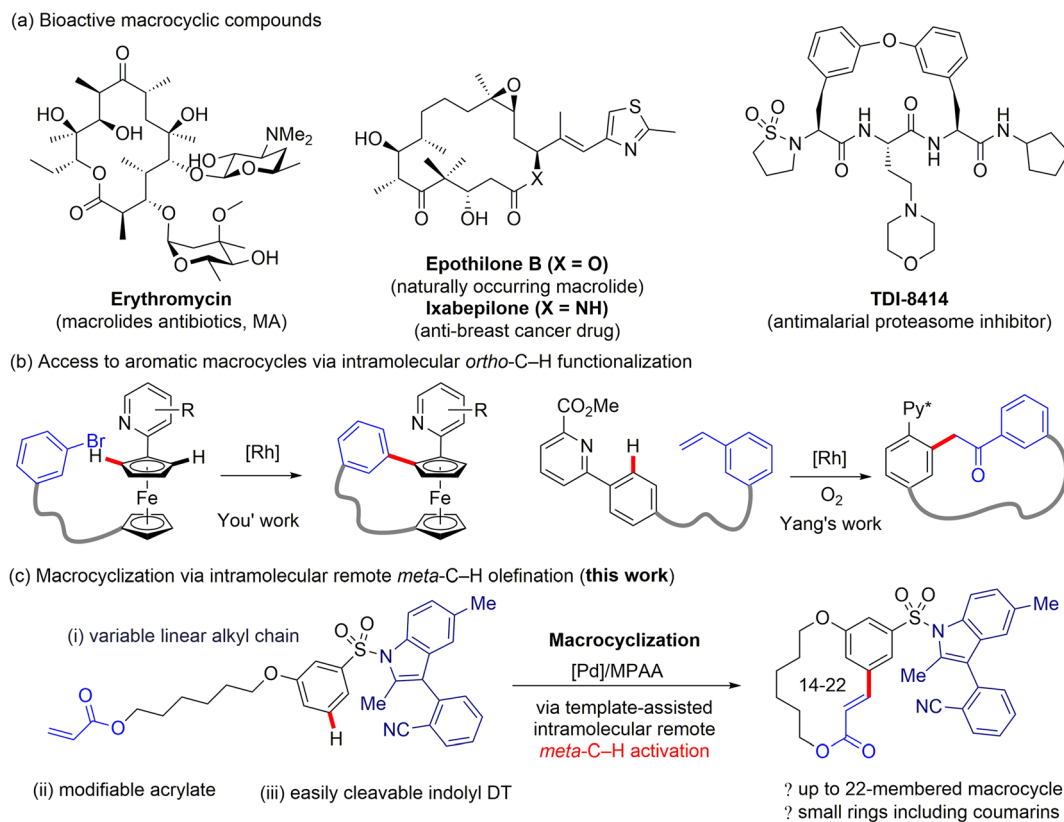


Fig. 1 Pharmaceutical importance of macrocyclic compounds and development of strategies for macrocyclization via C–H functionalization.

derivatives. However, the remote directed C–H bond functionalization of aryl sulfonic acids using reported templates¹² has been unsuccessful.^{5b,13} Competitive *ortho*-C–H functionalization directed by a secondary sulfonamide severely erodes remote C–H functionalization selectivity, and the inductive electron-withdrawing properties of the sulfonamide further reduces remote C(sp²)-H bond metalation reactivity. To overcome these challenges, a new highly site-selective directing template for intramolecular macrocyclization of aryl sulfonic acids must be developed.

Despite our extensive efforts in template development, we found the reported flexible DT cannot be used for the *meta*-C–H activation of aryl sulfonic acids. Template-enabled remote C–H functionalization of aryl sulfonate substrates is greatly impeded by the following major problems: the aryl sulfonate ester linkage is unstable; a secondary sulfonamide linkage effectively directs *ortho*-C–H functionalization;¹⁴ *N*-alkyl sulfonamide linkage is difficult to remove. It is well-known that the *N*-aryl sulfonyl protected indoles can be efficiently formed and cleaved under the relatively mild conditions, therefore, the aryl sulfonyl groups, e.g. *p*-tosyl, are shown to be a class of superior protecting group for the N–H bond of indoles.¹⁵ Given the practicality of *N*-aryl sulfonyl groups, we questioned whether a substituted indole scaffold can be engineered as a new remote DT for *meta*- or *para*-selective C–H functionalization of aryl sulfonates. Our recent statistical analyses suggested that site-selectivity of directed distal C–H functionalization are correlated with the MCP size and rigidity of DT.¹⁶ To test our

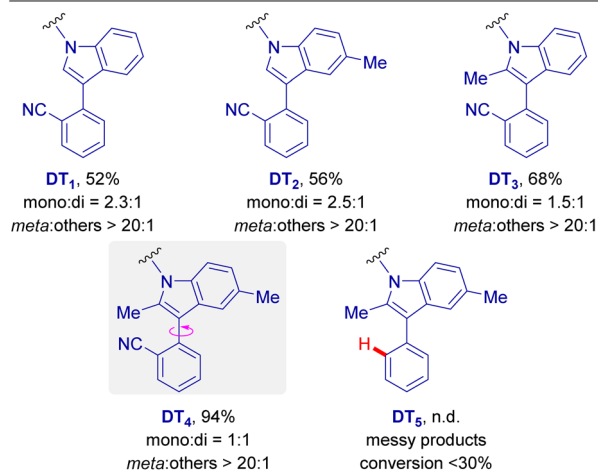
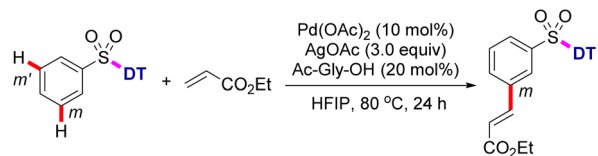
hypothesis, several nitrile-containing 3-arylindole derivatives were prepared and investigated for palladium-catalysed *meta*-C–H functionalization of aryl sulfonates. We herein disclose a rigid biaryl indole scaffold as the key template motif for intramolecular *meta*-selective C–H olefination of aryl sulfonate substrates (Fig. 1c). The indolyl template affords a 12-membered pre-transition state, the optimal MCP size for *meta* site-selection. The *N*-sulfonamide linkage is readily removable under mild conditions.

Results and discussion

Template design

In our efforts to develop a directing template for the remote C–H functionalization of benzenesulfonic acid derivatives, we initially prepared various nitrile-containing DTs containing 3-aryl indoles, which were then appended to the benzenesulfonic acid substrate via an *N*-sulfonamide linkage (Scheme 1). With ethyl acrylate as a coupling partner, exploratory studies on the palladium-catalysed remote *meta* C–H olefination of these benzenesulfonamide substrates were performed. Gratifyingly, with DT₁ as a directing template, C–H olefination afforded the desired product in 52% yield with >20:1 *meta* selectivity. Furthermore, the directing groups (DT₂ and DT₃) bearing a C5- or C2-methyl group on the indole moiety also yielded the corresponding *meta*-C–H olefinated products in 56% and 68% yield, respectively. It is worth noting that, with this type of indole scaffolds as the DT, all C–H olefination reactions provide



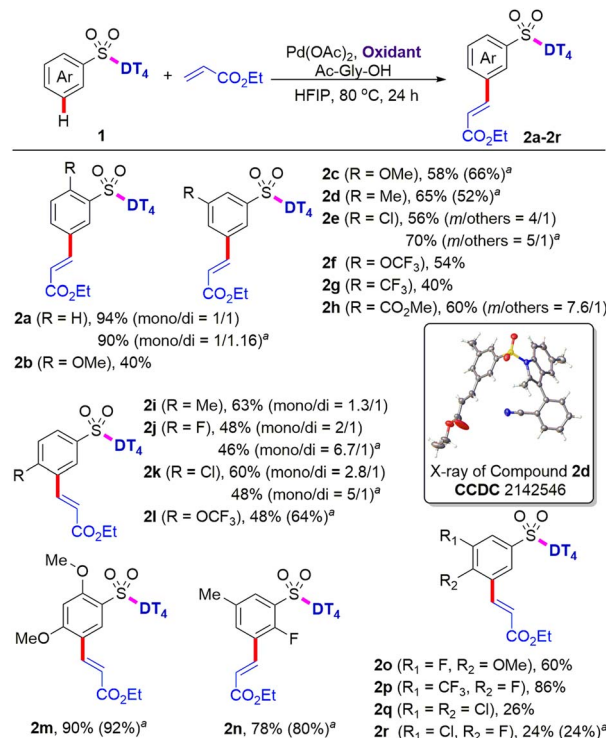


Scheme 1 Evaluation of DTs for *meta*-C–H functionalization of aryl sulfonic acids. Reaction conditions: PhSO₂-DT_{*n*} (0.1 mmol), ethyl acrylate (0.2 mmol), Pd(OAc)₂ (10 mol%), Ac-Gly-OH (20 mol%), AgOAc (0.3 mmol), HFIP (1.0 mL), 80 °C, 24 h. Yield, ratio of mono- and di-products and *meta* selectivity were determined by ¹H NMR analysis of the crude products with Cl₂CHCHCl₂ as an internal standard.

the target products in high *meta*-selectivity (*meta* : others > 20 : 1). Due to the fact that the starting materials was nearly consumed in all reactions, a thorough investigation on the side products was conducted. It was shown that C–H olefinations at C2 and C5 positions of the indole ring were the main side reactions, likely due to the electrophilic palladation on the electron-rich indole ring.¹⁷ Therefore, template (**DT₄**) incorporating two methyl groups into the C2 and C5 positions of indole ring was developed and subjected to the palladium-catalysed C–H olefination reaction. These improved templates delivered the C–H olefination products in 94% yield with exclusive *meta* selectivity (*meta* : others > 20 : 1). In contrast with transition metal-catalysed *ortho*-C–H functionalization, directed distal C–H bond functionalization commonly involves a conformationally variable macrocyclic transition state.^{5b} The presence of a C2 methyl group in the indole ring, apart from blocking the undesirable C–H palladation, also significantly prevents free rotation of atroposelective axis in the directing template (**DT₄**), likely beneficial to the formation of the conformationally rigid MCP-like pre-transition state.¹⁸ A control experiment omitting the nitrile group from the directing template (**DT₅**) results in less than 30% conversion and a complex mixture, validating that the coordinating nitrile is indispensable for *meta*-selective C–H activation.

Pd-catalysed *meta*-C–H olefination of aryl sulfonic acids

With the optimal DT in hand, we subsequently investigated the applicability of palladium-catalysed intermolecular *meta*-



Scheme 2 Scope of aryl sulfonic acids. Reaction conditions: ArSO₂-DT₄ **1** (0.1 mmol), ethyl acrylate (0.2 mmol), Pd(OAc)₂ (10 mol%), AgOAc (0.3 mmol), Ac-Gly-OH (20 mol%), HFIP (1.5 mL), 80 °C, 24 h. Isolated yields were reported. Ratio of mono- and di-products were determined by ¹H NMR spectra analysis of the crude products with Cl₂CHCHCl₂ as an internal standard. ^aIsolated yields when using Cu(OAc)₂ (0.05 mmol) and O₂ (1 atm) as the terminal oxidant.

selective C–H olefination (Scheme 2). It was found that substrates bearing the methoxy, methyl, and halo functional groups at *meta* or *para* position of benzenesulfonates were well tolerated under the present C–H olefination reaction conditions, providing the corresponding *meta* olefinated products (**2c–2e**, **2i–2k**) in 48–65% yields. Di-olefination occurred prominently with *para*-substituted benzenesulfonates to give the products (**2i–2k**). The *meta* selectivity of C–H olefination was comprehensively confirmed by X-ray diffraction analysis of product (**2d**).[‡] Reaction with substrate owning an *o*-OMe delivered the product (**2b**) in slightly decreased yield (40%), probably due to the steric repulsion between the methoxy group and tetrahedral sulfonate group, which disfavors the requisite *meta*-directing conformation. Given the existing electron-withdrawing sulphonamide motif, the incorporation of additional electron-withdrawing substituents might further deactivate the substrate towards C–H palladation. In contrast to this expectation and the reported reactivity trends for the remote *meta*-C–H functionalization of benzoic acids,¹² aryl sulfonamides bearing a diverse set of electron-withdrawing groups, such as trifluoromethoxy, trifluoromethyl, and ester groups at *meta* or *para* position, are all compatible, providing the desired products (**2f**, **2l**, **2g**, and **2h**) in 40–60% yields with exclusive *meta* selectivity. Di-substituted aryl sulfonates with different substitution patterns are also suitable for the directed *meta*-C–H



functionalization, successfully affording the tetra-substituted aryl sulfonates (**2m–2p**) in 60–90% yields. Reactions with 3,4-di-halo substituted aryl sulfonates were distinctly sluggish and the desired products (**2q** and **2r**) were isolated only in 26% and 24% yields, respectively. The reason for the stark contrast remains uncertain at this stage.

Given the high cost of excess silver acetate as the oxidant, the use of greener and more inexpensive oxidants is highly desirable. We found that 0.5 equiv. of copper acetate in combination with O₂ (1 atm) as the terminal oxidant (Scheme 2) also successfully provided the corresponding olefinated products (**2a**, **2c–2e**, **2j–2n**, and **2r**) in comparable yields. These results indicate that Ag salts can be replaced as oxidants in directing template-assisted remote C–H functionalization (*vide infra*).

After the survey of scope with aryl sulfonates, the established template-directed *meta*-C–H functionalization was then extended to other olefin partners (Scheme 3). In addition to ethyl acrylate, other alkyl ester (**3a**) are also suitable substrates for this C–H olefination reaction. Methyl crotonate and methyl cinnamate are compatible under the reaction conditions, giving the desired products (**3e** and **3f**) in 47% and 86% yields, respectively. Likewise, other activated olefins, *i.e.*, vinyl amide and vinyl sulfonates, can also be employed to the present process, providing the corresponding products (**3b–3d**) in 68–82% yields. Furthermore, C–H olefination with cyclic α,β -unsaturated esters smoothly provided the related products (**3g** and **3h**) in good to excellent yields with exclusive *meta* selectivity. Electron-deficient perfluorinated olefin is

demonstrated to be competent substrate, affording the 3,5-disubstituted perfluoroalkenylated product (**3j**) in 80% yield. In particular, coupling with olefins containing the biologically significant natural terpenes, *e.g.* estrone, L-menthol, and stanolone, successfully produced the mono- or di-olefinated products (**3i**, **3k** and **3l**) in 56–72% yields, which is highly applicable for synthesis of a diverse range of pharmaceutical conjugates.

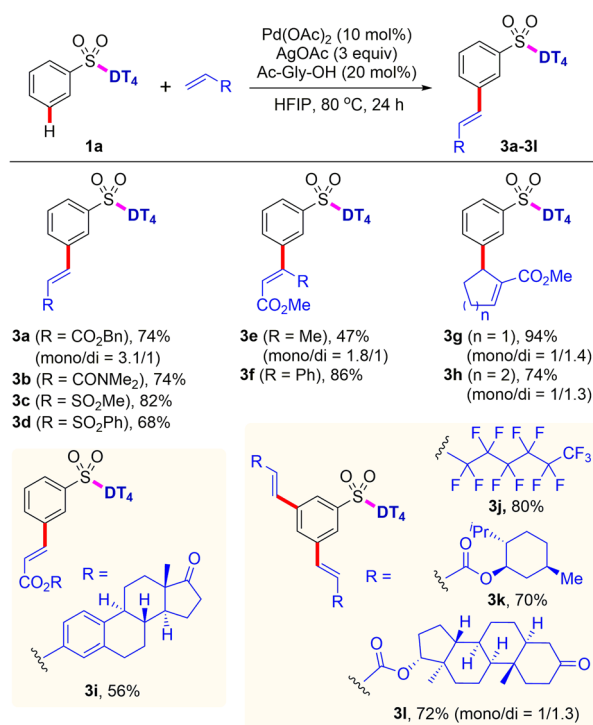
Macrocyclization *via* intramolecular *meta*-C–H olefination

Having successfully realized *meta*-C–H functionalization of aryl sulfonic acids, we revisited our initial proposal to synthesize aromatic macrocycles using palladium-catalysed intramolecular remote *meta*-selective C–H olefination. Pleasingly, we found that the macrocyclization of **4c** proceeds successfully to generate an 18-membered macrolide product **5c** in satisfied yield under the optimized conditions of 10 mol% Pd(OAc)₂ catalyst, 20 mol% N-Ac-Gly-OH ligand and 3 equiv. of AgOAc in hexafluoroisopropanol (HFIP) at 60 °C for 1.5 h (see ESI† for detailed reaction conditions optimization), although some competitive intermolecular reaction was observed. It was found that the highest yield (68%) was achieved when macrocyclization reaction was conducted at a 25 mM concentration. With the decrease of Pd catalyst from 10 mol% to 2 mol%, the isolated yield of **5c** is reduced to 34%. Extended reaction times did not bring about higher yields. When reaction was carried out over a period of 24 h, no desired macrocyclization product was observed, suggesting macrocycle decomposition under long reaction times. The NMR spectra and HPLC/MS analyses indicate that the hydrolysis of lactone occurred, leading to the formation of the corresponding cinnamic acids in the presence of a small amount of H₂O in HFIP.

Next, we further investigated the generality of template-enabled macrocyclization methodology (Scheme 4). We were pleased to find the present method demonstrated the considerable tolerance of macrocycle sizes. Under the optimized conditions, by using the different chain lengths of alkyl groups, all of 14- to 22-membered macrolides **5a–5e** can be smoothly obtained in 42–68% yields. The macrocyclization protocol was also compatible with the different acrylate tails, for example cinnamates **5h** and **5i**, albeit in decreased yields. Notably, the use of α -methyl acrylate derivative caused that a macrocycle **5f** with exocyclic double bond was isolated as the major product.

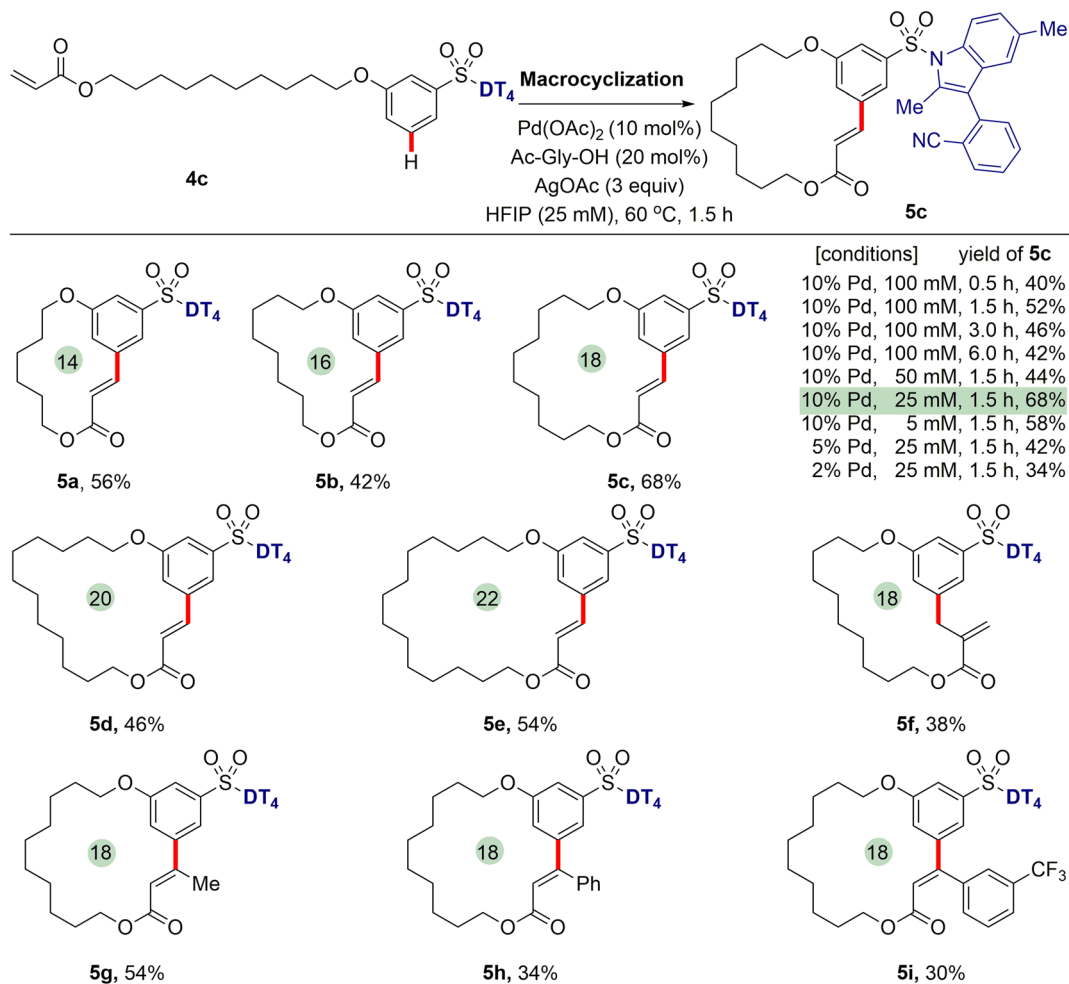
Synthetic utility of *meta*-C–H functionalization

Encouraged by our success with the Pd-catalysed macrocyclization *via* intramolecular *meta*-C–H olefination, we then sought to apply our strategy to the template-directed intramolecular *meta*-selective C–H functionalization to prepare small ring compounds, such as coumarins, which has yet to be reported.^{1c} Pleasingly, assisted with directing template DT₄, Pd-catalysed intramolecular *meta*-C–H olefination smoothly afforded the 6-sulfonate group-substituted coumarin (**7**) in 46% yield by using the linear precursor acrylates (**6**) as the starting substrate (Scheme 5a).



Scheme 3 Scope of olefins for intermolecular *meta*-C–H functionalization. Reaction conditions: PhSO₂-DT₄ **1a** (0.1 mmol), olefin (0.2 mmol), Pd(OAc)₂ (10 mol%), AgOAc (0.3 mmol), Ac-Gly-OH (20 mol%), HFIP (1.5 mL), 80 °C, 24 h. Isolated yields were reported.





Scheme 4 Macrocyclization via template-directed intramolecular remote *meta*-C–H olefination. Reaction conditions: ArSO₂-DT₄ **4** (0.1 mmol), Pd(OAc)₂ (10 mol%), AgOAc (0.3 mmol), Ac-Gly-OH (20 mol%), HFIP (25 mM), 60 °C, 1.5 h. Isolated yields were reported.

To further test the practicality of template-enabled *meta*-C–H functionalization of aryl sulfonate derivatives, an antitumor drug Belinostat **9**, also known as a pan-histone deacetylase (HDAC) inhibitor, was concisely synthesized through using the established C–H olefination method (Scheme 5b). After further optimization of reaction parameters, a slightly higher ratio (1.4 : 1) of mono- vs. di-products was achieved when using 1.5 equivalents of ethyl acrylate over 6 h reaction time for preparation of key intermediate **2a_{mono}**. Finally, belinostat **9** was synthesized in a five-step sequence with an overall yield of 22% from the inexpensive readily available PhSO₂Cl.

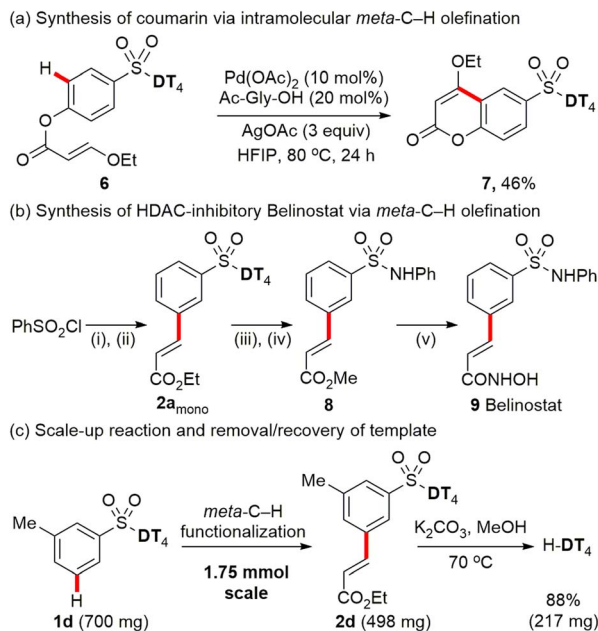
Furthermore, we also successfully scaled up the reaction to 1.75 mmol (Scheme 5c). Palladium-catalysed *meta*-C–H olefination of aryl sulfonate **1d** provides the target mono-product **2d** in 57% isolated yield. The directing template DT₄ is readily removed under mild conditions (K₂CO₃, MeOH) and recovered in 88% isolated yield.

Mechanistic study

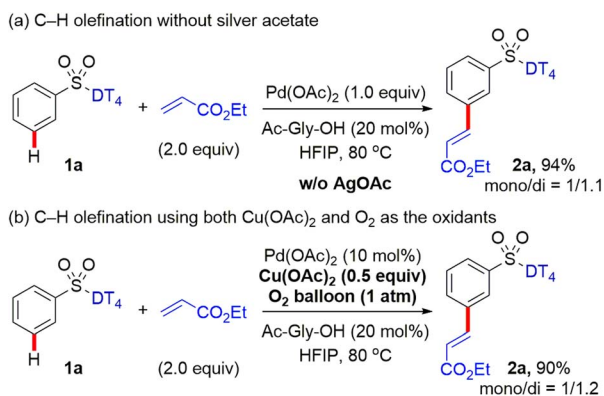
For the previously reported Pd-catalysed *meta*-selective C–H functionalization of arene substrates, such as 3-hydrocinnamic

acids⁴ and distal arene-tethered aliphatic alcohols,^{6h} using nitrile-based DT, silver acetate was often indispensable for the catalytic process. Earlier mechanistic studies indicated Ag salts not only serve as an external oxidant, but also participate the assembly of MCP-like pre-transition state, crucial for the desired positional selectivity. Density functional theory (DFT) studies¹³ indicated that heterodimeric PdAg(OAc)₃ as the active catalytic species is likely involved in the key C–H activation step. In the hypothetical transition state, the DG nitrile coordinates to Ag while the acetate-bridged Pd is located close to the *meta* C–H bond, thereby accounting for the high site selectivity. To examine the role of silver acetate in the present C–H functionalization, the *meta*-selective C–H olefination of aryl sulfonates was performed by employing the stoichiometric Pd catalyst, and the comparable site-selectivity and ratio of mono : di products were observed, indicated that AgOAc likely only acts as an external oxidant for this transformation (Scheme 6a). To provide additional support for this proposal, the reaction was also performed when using catalytic Cu(OAc)₂ (0.5 equiv.) and O₂ (1 atm) as the oxidant system (Scheme 6b) as in our study above (Scheme 2). The yield and *meta*-selectivity are nearly identical as when using AgOAc as the oxidant (Scheme 2).



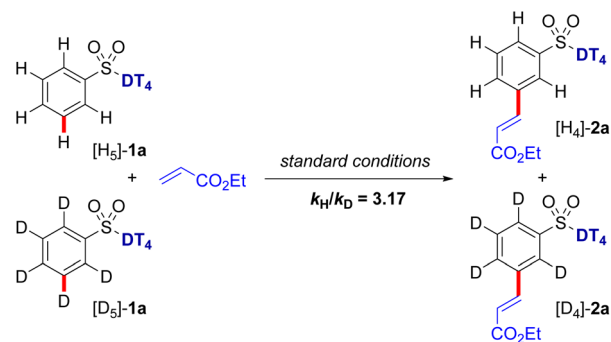


Scheme 5 Synthetic application of Pd-catalysed *meta*-C–H functionalization. Reaction conditions: (i) H-DT₄ (1.1 equiv.), NaH, THF, 90%; (ii) PhSO₂-DT₄ **1a** (1 equiv.), ethyl acrylate (1.5 equiv.), Pd(OAc)₂ (10 mol%), AgOAc (3 equiv.), Ac-Gly-OH (20 mol%), HFIP (1.5 mL), 80 °C, 6 h, 54% yield for **2a_{mono}**, 38% yield for **2a_{di}**; (iii) K₂CO₃, MeOH; then aq. HCl; then MeI, K₂CO₃, DMF, rt. (iv) SOCl₂, DMF (cat), toluene; then aniline, pyridine, rt, 70% overall yield from compound **2a_{mono}**. (v) aq. NaOH, MeOH, rt; then SOCl₂, DBU (cat); then NH₂OH·HCl, aq. NaHCO₃, 65% overall yield from compound **8**.



Scheme 6 Pd-catalysed *meta*-C–H olefination under the variable conditions.

Kinetic isotope effect (KIE) studies on the C–H olefination of **1a** and its deuterated analog [D₅]-**1a** provided k_H/k_D value of 3.17 (Scheme 7), implying that the C–H bond cleavage is likely the rate-determining step (RDS) in the catalytic cycle. To gain further mechanistic insights into the catalytic cycle, we also performed a series of control experiments and spectroscopic analyses. In the absence of the Pd catalyst, no desired olefination products were detected. When the N-protected amino acid ligand was omitted (N-Ac-Gly-OH), a sluggish reaction was observed. Subsequently, kinetic studies were carried out to



Scheme 7 Kinetic isotope effect experiment.

determine the reaction order with respect to the aryl sulfonate substrate and olefin coupling partner (see Fig. S2 and S3 in ESI†). From the initial rate calculations, a first-order rate dependency with respect to aryl sulfonate and zero-order dependency with respect to the olefin were obtained. The observed first order rate dependency on the aryl sulfonate substrate indicates the C–H activation step is the rate-limiting step, consistent with the KIE results.

Upon coordination of the nitrile N atom to the Pd catalyst in the directed distal C–H activation, the stretching vibrational frequency ($\nu_{\text{C}\equiv\text{N}}$) of carbon–nitrogen triple bond on the nitrile group changes dramatically. To detect the possible reaction

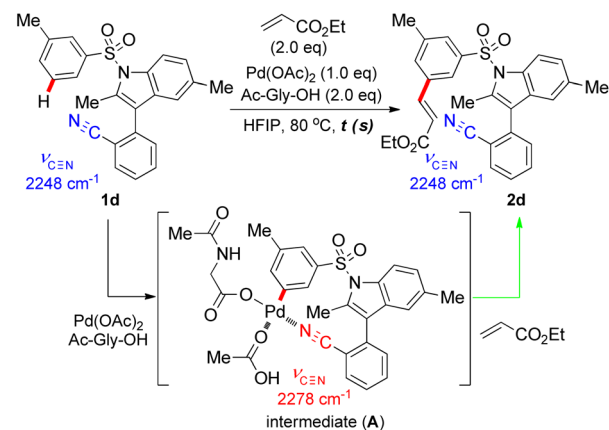
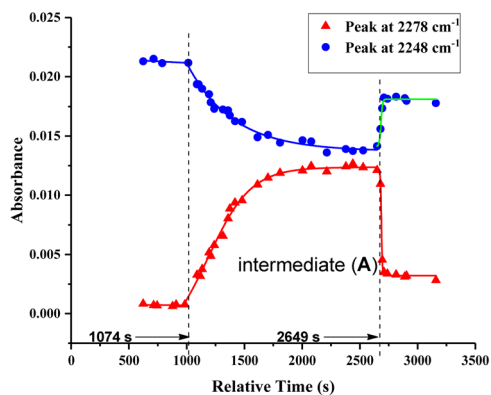


Fig. 2 *In situ* IR reaction kinetic profiles.



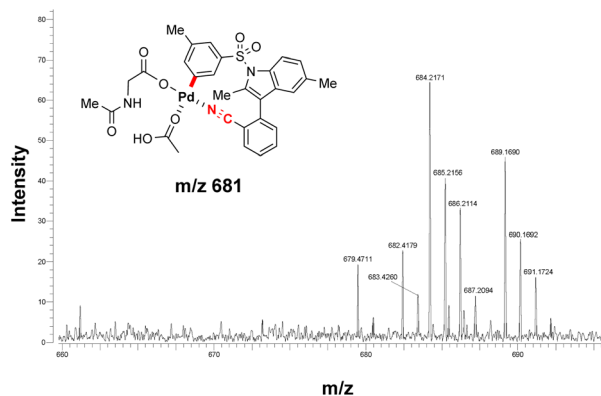


Fig. 3 ESI-MS spectra analysis to detect the PdL_n-arene complex with substrate **1d**.

intermediate in this remote C–H functionalization reaction, *in situ* Fourier-transform infrared (*in situ* FTIR) was employed to monitor the reaction with the substrate **1d**, stoichiometric Pd catalysts and N-Ac-Gly-OH ligand. From the kinetic profile of the intermediate concentration *versus* time (ConcIRT), apart from aryl sulfonate substrate and the desired olefinated product (both typical absorbance peak at 2248 cm⁻¹), we observed a new active species (absorbance peak at 2278 cm⁻¹), which probably corresponds to the MCP-like assembly (Fig. 2). When the stoichiometric Pd(OAc)₂ and N-Ac-Gly-OH ligand was added into

the solution of substrate in hexafluoroisopropanol (HFIP), aryl sulfonate **1d** was consumed promptly and a new intermediate (**A**) was generated (absorbance peak at 2278 cm⁻¹) within 30 minutes. Subsequently, after the introduction of ethyl acrylate, the absorbance peak at 2278 cm⁻¹ subsided instantly, accompanied by the rapid formation of C–H olefination products (also absorbance peak at 2248 cm⁻¹).

ESI-MS studies of the reaction mixture, in the absence of the olefinated reagent, also detected the formation of an MCP-like palladacycle as illustrated in Fig. 3. Identification of this active intermediate, as well as its rate of consumption upon the addition of olefin, represents valuable mechanistic information on template directed C–H activation reactions.

In combination with *in situ* IR spectroscopic analysis and earlier reports^{13,19} on Pd-catalysed *meta*-C–H activation, a putative catalytic mechanism for the present template-assisted C–H functionalization was therefore proposed (Fig. 4). As shown in the intermediate **II**, the directing template directs the Pd center to the distal aryl C–H bond with the appropriate distal and geometric arrangement. Next, *meta*-selective C–H activation, proceeding *via* a ligand-assisted concerted metalation-deprotonation (CMD) mechanism,²⁰ forms an MCP-like palladated intermediate (**A**). In the presence of olefin partner, migratory insertion of olefin, followed by sequential β-hydride elimination of the resulting intermediate **IV**, provides the desired *meta*-C–H olefinated products.

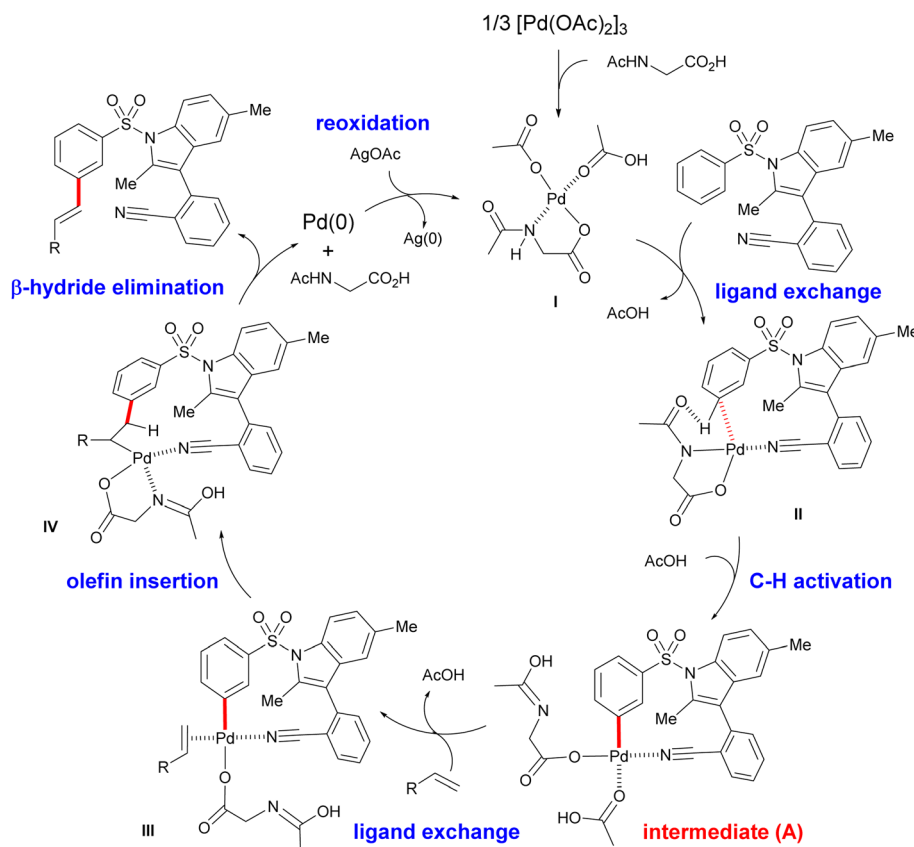


Fig. 4 A plausible catalytic cycle.



Conclusions

In summary, Pd-catalysed macrocyclization *via* remote intramolecular *meta*-C–H olefination was successfully achieved by utilizing an indolyl DT. The synthetic utility of the strategy was demonstrated in synthesis of a series of macrolides with different scaffold sizes. In addition, application to the concise synthesis of anti-tumor drug Belinostat validates the method's compatibility with intermolecular *meta*-C–H functionalization as well. Through *in situ* IR profiling, ESI-MS studies, and kinetic experiments, we provide the first experimental support for the formation of an active macrocyclic palladacycle intermediate from remote C–H activation.

Data availability

The datasets supporting this article have been uploaded as part of the ESI† material.

Author contributions

X. X., Z. J., and J.-Q. Y. conceptualized the project. P. Z., Z.-W. J., G. L., Q. M., J. H., and J. T. performed the experimental studies. Z. J., Z. F., and J.-Q. Y. prepared the manuscript.

Conflicts of interest

There are no conflicts to declare.

Acknowledgements

Financial support from the National Natural Science Foundation of China (No. 22171145 to Z. J. and 32072440 to X. X.) is gratefully acknowledged. The authors thank Dr Kevin Wu for extensive proofreading.

Notes and references

‡ Deposition number 2142546 (for compound **2d**) contains the supplementary crystallographic data for this paper. These data are provided free of charge by the joint Cambridge Crystallographic Data Centre.

- (a) K. Godula and D. Sames, *Science*, 2006, **312**, 67; (b) X. Chen, K. M. Engle, D.-H. Wang and J.-Q. Yu, *Angew. Chem., Int. Ed.*, 2009, **48**, 5094; *Angew. Chem.*, 2009, **121**, 5196; (c) L. McMurray, F. O'Hara and M. J. Gaunt, *Chem. Soc. Rev.*, 2011, **40**, 1885; (d) S. R. Neufeldt and M. S. Sanford, *Acc. Chem. Res.*, 2012, **45**, 936; (e) J. F. Hartwig, *J. Am. Chem. Soc.*, 2016, **138**, 2.
- (a) O. Daugulis, H. Q. Do and D. Shabashov, *Acc. Chem. Res.*, 2009, **42**, 1074; (b) T. W. Lyons and M. S. Sanford, *Chem. Rev.*, 2010, **110**, 1147; (c) D. A. Colby, R. G. Bergman and J. A. Ellman, *Chem. Rev.*, 2010, **110**, 624; (d) D. A. Colby, A. S. Tsai, R. G. Bergman and J. A. Ellman, *Acc. Chem. Res.*, 2012, **45**, 814; (e) G. Rouquet and N. Chatani, *Angew. Chem., Int. Ed.*, 2013, **52**, 11726; *Angew. Chem.*, 2013, **125**, 11942; (f) K. M. Engle, T.-S. Mei, M. Wasa and J.-Q. Yu, *Acc. Chem. Res.*, 2012, **45**, 788; (g) L. Ackermann, *Acc. Chem. Res.*, 2014, **47**, 281.
- (a) F. Juliá-Hernández, M. Simonetti and I. Larrosa, *Angew. Chem., Int. Ed.*, 2013, **52**, 11458; *Angew. Chem.*, 2013, **125**, 11670; (b) J. Ye and M. Lautens, *Nat. Chem.*, 2015, **7**, 863; (c) J. Li, S. De Sarkar and L. Ackermann, *Top. Organomet. Chem.*, 2015, **55**, 217; (d) M. T. Mihai, G. R. Genov and R. J. Phipps, *Chem. Soc. Rev.*, 2018, **47**, 49.
- D. Leow, G. Li, T.-S. Mei and J.-Q. Yu, *Nature*, 2012, **486**, 518.
- (a) A. Dey, S. K. Sinha, T. K. Achar and D. Maiti, *Angew. Chem., Int. Ed.*, 2019, **58**, 10820; *Angew. Chem.*, 2019, **131**, 10934; (b) G. Meng, N. Y. S. Lam, E. L. Lucas, T. G. Saint-Denis, P. Verma, N. Chekshin and J.-Q. Yu, *J. Am. Chem. Soc.*, 2020, **142**, 10571; (c) W. Ali, G. Prakash and D. Maiti, *Chem. Sci.*, 2021, **12**, 2735; (d) U. Dutta, S. Maiti, T. Bhattacharya and D. Maiti, *Science*, 2021, **372**, eabd5992; (e) Z. Fan, X. Chen, K. Tanaka, H. S. Park, N. Y. S. Lam, J. J. Wong, K. N. Houk and J.-Q. Yu, *Nature*, 2022, **610**, 87.
- (a) H.-X. Dai, G. Li, X.-G. Zhang, A. F. Stepan and J.-Q. Yu, *J. Am. Chem. Soc.*, 2013, **135**, 7567; (b) S. Lee, H. Lee and K. L. Tan, *J. Am. Chem. Soc.*, 2013, **135**, 18778; (c) R.-Y. Tang, G. Li and J.-Q. Yu, *Nature*, 2014, **507**, 215; (d) G. Yang, P. Lindovska, D. Zhu, J. Kim, P. Wang, R.-Y. Tang, M. Movassaghi and J.-Q. Yu, *J. Am. Chem. Soc.*, 2014, **136**, 10807; (e) L. Chu, M. Shang, K. Tanaka, Q. Chen, N. Pissarnitski, E. Streckfuss and J.-Q. Yu, *ACS Cent. Sci.*, 2015, **1**, 394; (f) M. Bera, A. Maji, S. K. Sahoo and D. Maiti, *Angew. Chem., Int. Ed.*, 2015, **54**, 8515; *Angew. Chem.*, 2015, **127**, 8635; (g) S. Bag, R. Jayarajan, U. Dutta, R. Chowdhury, R. Mondal and D. Maiti, *Angew. Chem., Int. Ed.*, 2017, **56**, 12538; *Angew. Chem.*, 2017, **129**, 12712; (h) L. Zhang, C. Zhao, Y. Liu, J. Xu, X. Xu and Z. Jin, *Angew. Chem., Int. Ed.*, 2017, **56**, 12245; *Angew. Chem.*, 2017, **129**, 12413; (i) Z. Zhang, K. Tanaka and J.-Q. Yu, *Nature*, 2017, **543**, 538; (j) S. Li, H. Wang, Y. Weng and G. Li, *Angew. Chem., Int. Ed.*, 2019, **58**, 18502; *Angew. Chem.*, 2019, **131**, 18673; (k) S. Porey, X. Zhang, S. Bhowmick, V. K. Singh, S. Guin, R. S. Paton and D. Maiti, *J. Am. Chem. Soc.*, 2020, **142**, 3762; (l) A. F. Williams, A. J. P. White, A. C. Spivey and C. J. Cordier, *Chem. Sci.*, 2020, **11**, 3301; (m) S. Bag, S. Jana, S. Pradhan, S. Bhowmick, N. Goswami, S. K. Sinha and D. Maiti, *Nat. Commun.*, 2021, **12**, 1393; (n) S. Bag, T. Patra, A. Modak, A. Deb, S. Maity, U. Dutta, A. Dey, R. Kancherla, A. Maji, A. Hazra, M. Bera and D. Maiti, *J. Am. Chem. Soc.*, 2015, **137**, 11888; (o) A. Maji, A. Dahiya, G. Lu, T. Bhattacharya, M. Brochetta, G. Zanoni, P. Liu and D. Maiti, *Nat. Commun.*, 2018, **9**, 3582; (p) X. Chen, S. Fan, M. Zhang, Y. Gao, S. Li and G. Li, *Chem. Sci.*, 2021, **12**, 4126; (q) P. Ramesh, C. Sreenivasulu, D. R. Kishore, D. Srinivas, K. R. Gorantla, B. S. Malik and G. Satyanarayana, *J. Org. Chem.*, 2022, **87**, 2204; (r) A. Saha, S. Guin, W. Ali, T. Bhattacharya, S. Sasmal, N. Goswami, G. Prakash, S. K. Sinha, H. B. Chandrashekar, S. Panda, S. S. Anjana and D. Maiti, *J. Am. Chem. Soc.*, 2022, **144**, 1929.
- (a) E. M. Driggers, S. P. Hale, J. Lee and N. K. Terrett, *Nat. Rev. Drug Discovery*, 2008, **7**, 608; (b) E. Marsault and



- M. L. Peterson, *J. Med. Chem.*, 2011, **54**, 1961; (c) T. A. F. Cardote and A. Ciulli, *ChemMedChem*, 2016, **11**, 787.
- 8 (a) J. R. Frost, C. C. G. Scully and A. K. Yudin, *Nat. Chem.*, 2016, **8**, 1105; (b) X. Zhang, G. Lu, M. Sun, M. Mahankali, Y. Ma, M. Zhang, W. Hua, Y. Hu, Q. Wang, J. Chen, G. He, X. Qi, W. Shen, P. Liu and G. Chen, *Nat. Chem.*, 2018, **10**, 540; (c) C.-X. Liu, P.-P. Xie, F. Zhao, Q. Wang, Z. Feng, H. Wang, C. Zheng and S.-L. You, *J. Am. Chem. Soc.*, 2023, **145**, 4765; (d) B. Song, X. Guo, L. Yang, H. Yu, X. Zong, X. Liu, H. Wang, Z. Xu, Z. Lin and W. Yang, *Angew. Chem., Int. Ed.*, 2023, e202218886.
- 9 S. Sengupta and G. Mehta, *Org. Biomol. Chem.*, 2020, **18**, 1851.
- 10 K. T. Mortensen, T. J. Osberger, T. A. King, H. F. Sore and D. R. Spring, *Chem. Rev.*, 2019, **119**, 10288.
- 11 U. Lücking, G. Siemeister, M. Schäfer, H. Beiem, M. Krüger, P. Lienau and R. Jautelat, *ChemMedChem*, 2007, **2**, 63.
- 12 (a) S. Li, L. Cai, H. Ji, L. Yang and G. Li, *Nat. Commun.*, 2016, **7**, 10443; (b) L. Fang, T. G. Saint-Denis, B. L. H. Taylor, S. Ahlquist, K. Hong, S. Liu, L. Han, K. N. Houk and J.-Q. Yu, *J. Am. Chem. Soc.*, 2017, **139**, 10702.
- 13 (a) Y.-F. Yang, G.-J. Cheng, P. Liu, D. Leow, T.-Y. Sun, P. Chen, X. Zhang, J.-Q. Yu and Y.-D. Wu, *J. Am. Chem. Soc.*, 2014, **136**, 344; (b) Z. Fan, K. L. Bay, X. Chen, Z. Zhuang, H. S. Park, K.-S. Yeung, K. N. Houk and J.-Q. Yu, *Angew. Chem., Int. Ed.*, 2020, **59**, 4770; *Angew. Chem.*, 2020, **132**, 4800.
- 14 (a) M. V. Pham, B. Ye and N. Cram, *Angew. Chem., Int. Ed.*, 2012, **51**, 10610; *Angew. Chem.*, 2012, **124**, 10762; (b) Y. Ran, Y. Yang, H. You and J. You, *ACS Catal.*, 2018, **8**, 1796; (c) Y. Dong, X. Zhang, J. Chen, W. Zou, S. Lin and H. Xu, *Chem. Sci.*, 2019, **10**, 8744; (d) H.-X. Dai, A. F. Stepan, M. S. Plummer, Y.-H. Zhang and J.-Q. Yu, *J. Am. Chem. Soc.*, 2011, **133**, 7222; (e) G. Wu, W. Ouyang, Q. Chen, Y. Huo and X. Li, *Org. Chem. Front.*, 2019, **6**, 284; (f) T. Lan, L. Wang and Y. Rao, *Org. Lett.*, 2017, **19**, 972; (g) S. Rej and N. Chatani, *Chem. Sci.*, 2020, **11**, 389; (h) W. Liu, D. Wang, Y. Zhao, F. Yi and J. Chen, *Adv. Synth. Catal.*, 2016, **358**, 1968; (i) S. Feng, S. Li, J. Li and J. Wei, *Org. Chem. Front.*, 2019, **6**, 517; (j) S. Ojha and N. Panda, *Adv. Synth. Catal.*, 2020, **362**, 561.
- 15 P. G. M. Wuts and T. W. Greene, *Greene's Protective Groups in Organic Synthesis*, Wiley-Interscience, New Jersey, 4th edn, 2007.
- 16 N. Y. S. Lam, Z. Fan, K. Wu, H. S. Park, S. Y. Shim, D. A. Strassfeld and J.-Q. Yu, *J. Am. Chem. Soc.*, 2022, **144**, 2793.
- 17 A. H. Sandtorv, *Adv. Synth. Catal.*, 2015, **357**, 2403.
- 18 J. Xu, J. Chen, F. Gao, S. Xie, X. Xu, Z. Jin and J.-Q. Yu, *J. Am. Chem. Soc.*, 2019, **141**, 1903.
- 19 G.-J. Cheng, Y.-F. Yang, P. Liu, P. Chen, T.-Y. Sun, G. Li, X. Zhang, K. N. Houk, J.-Q. Yu and Y.-D. Wu, *J. Am. Chem. Soc.*, 2014, **136**, 894.
- 20 (a) D. Lapointe and K. Fagnou, *Chem. Lett.*, 2010, **39**, 1118; (b) L. Ackermann, *Chem. Rev.*, 2011, **111**, 1315.

